



# Melting of dehydrated oceanic crust from the stagnant slab and of the hydrated mantle transition zone: Constraints from Cenozoic alkaline basalts in eastern China



Tetsuya Sakuyama <sup>a,\*</sup>, Wei Tian <sup>b</sup>, Jun-Ichi Kimura <sup>a</sup>, Yoshio Fukao <sup>a</sup>, Yuka Hirahara <sup>a</sup>, Toshiro Takahashi <sup>a</sup>, Ryoko Senda <sup>a</sup>, Qing Chang <sup>a</sup>, Takashi Miyazaki <sup>a</sup>, Masayuki Obayashi <sup>a</sup>, Hiroshi Kawabata <sup>d</sup>, Yoshiyuki Tatsumi <sup>c</sup>

<sup>a</sup> Institute for Research on Earth Evolution, Japan Agency for Marine–Earth Science and Technology, 2-15 Natsushima-cho, Yokosuka 237-0061, Japan

<sup>b</sup> Key Laboratory of Orogenic Belts and Crustal Evolution, MOE, School of Earth and Space Sciences, Peking University, Beijing 100871, China

<sup>c</sup> Department of Earth and Planetary Sciences, Kobe University, Nada, Kobe 657-8501, Japan

<sup>d</sup> Research and Education Faculty, Multidisciplinary Science Cluster, Interdisciplinary Science Unit, Kochi University, Kochi 780-8520, Japan

## ARTICLE INFO

### Article history:

Received 3 August 2012

Received in revised form 19 September 2013

Accepted 24 September 2013

Available online 3 October 2013

Editor: L. Reisberg

### Keywords:

Intraplate alkaline basalt  
Eastern China  
Shandong Peninsula  
Silica-deficient basalt  
Stagnant Pacific slab  
Oceanic crust melting

## ABSTRACT

The feasibility of oceanic igneous crust melting in stagnant slabs has previously been proposed from experimental petrological research. However, geochemical evidence for such melting has not yet been found from igneous rocks. We present evidence to suggest that melts from the igneous layer in the stagnant Pacific slab contributed to the source composition of basalts erupted in eastern China. Fe-rich (>13 wt.%), Si-poor (<43 wt.%) basalts occur only above the leading edge of the stagnant Pacific slab in eastern China, ~2000 km west of the Pacific Plate trench. The source of these basalts has Nd–Hf and Sr–Nd–Pb isotopic compositions akin to those of the igneous layer in the Pacific slab, and their extremely low Rb and Pb contents suggest that their source material was modified by subduction processes. Together with forward modeling calculation on trace elements and isotope compositions, these geochemical characteristics imply that they received a contribution from fluid released from hydrated transition zone and dehydrated carbonate-bearing oceanic crust in the stagnant slab, without a long time-integrated ingrowth of Sr–Nd–Hf–Pb isotope systems, almost at the leading edge of the stagnant Pacific slab.

© 2013 Elsevier B.V. All rights reserved.

## 1. Introduction

### 1.1. Presence of a stagnant slab and associated magmatism

Cold oceanic plates begin to sink along subduction zones and the constituent layers (both igneous and sedimentary) dehydrate and melt as they undergo subduction, feeding slab components to arc magmas (Gill, 1981). After subduction, the remaining cold slab reaches the mantle transition zone (at depths of 400–600 km), where its minerals undergo pressure-induced transformations. A delay in density changes by such transformations (resulting from the slab having a lower temperature than the surrounding mantle) sometimes prevents further slab penetration, causing the cold slab to stagnate (Ringwood and Irifune, 1988) in the mantle transition zone. Stagnation of the subducted Pacific slab in the mantle transition zone has been imaged

by seismic tomography (e.g., Fukao et al., 1992). Late Cenozoic (0–15 Ma) basalt volcanoes lying above the stagnant slab, are distributed throughout eastern China (e.g., Fan and Hooper, 1991). These basalts are rich in alkaline and incompatible trace elements that are typically associated with oceanic island basalts (OIBs). Such geochemical similarities between the basalts in eastern Asia and typical OIBs have led some researchers to conclude that the Chinese basalts originated from the upwelling of mantle, independent of a stagnant slab (Nakamura et al., 1985; Niu, 2005; Sakuyama et al., 2009; Zeng et al., 2011), while others believe that they were produced by or related to chemical components derived from the stagnant slab (Tatsumi and Eggins, 1995; Huang and Zhao, 2006; Richard and Iwamori, 2010; Kuritani et al., 2011).

Kuritani et al. (2011) first presented geochemical evidence for a hydrous mantle plume upwelling beneath Changbaishan in northeastern China, suggesting that the plume was fed by fluid dehydrated from sediments overlying the stagnant Pacific slab. According to the results of high-pressure experiments, melting of the stagnant slab (which affects slab chemistry and density more than dehydration) could occur if the slab contains adequate amounts of H<sub>2</sub>O or CO<sub>2</sub> (Dasgupta et al., 2004; Litasov and Ohtani, 2009; Dasgupta and Hirschmann, 2010). However, geochemical examination of the melting of the stagnant slab

\* Corresponding author at: 2-15 Natsushima-cho, Yokosuka-City, Kanagawa 237-0061, Japan. Tel.: +81 46 867 9785; fax: +81 46 867 9625.

E-mail address: [sakuyama@jamstec.go.jp](mailto:sakuyama@jamstec.go.jp) (T. Sakuyama).

has not yet been conducted, owing to the difficulty in identifying the signature of deep (>400 km) processes from surface manifestations.

## 1.2. Off-arc region of northeastern Asia

Seismic tomographic images show the presence of a high-velocity slab at depths of 410–660 km in eastern China, with a low-velocity

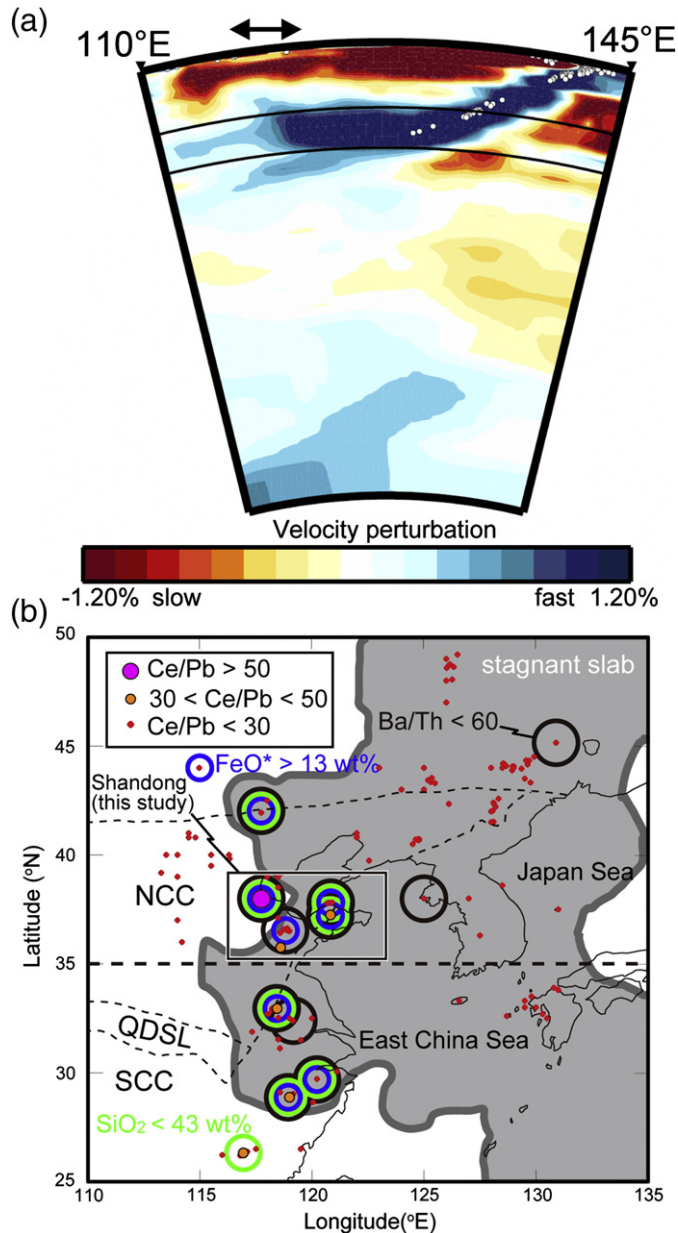


**Fig. 1.** Spatial distribution of Cenozoic basalts and vertical cross section of P-wave velocity tomography under northeast Asia. (a) East-west vertical cross section of P-wave velocity perturbation image along the profile shown as a thick broken line in (b). The range of longitude for which lavas exhibit low  $\text{SiO}_2$ , low  $\text{Al}_2\text{O}_3$ , high  $\text{FeO}^*$  contents, and high  $\text{Ce/Pb}$ , is shown by a black arrow. (b) Distribution of Cenozoic basalts with less differentiated compositions ( $\text{SiO}_2 < 60$  wt.% and  $\text{FeO}^*/\text{MgO} < 1.3$ ). Localities where samples with low  $\text{SiO}_2$  and high  $\text{FeO}^*$  contents and a low  $\text{Ba/Th} (<60)$  were reported are encircled by thick light-green, blue, and black circles respectively. Localities where samples with extremely high  $\text{Ce/Pb} (>50)$  and intermediately high  $\text{Ce/Pb}$  are plotted by large pink, and orange circles respectively. The western edge of the 0.3–0.6% P-wave high-velocity anomaly at a depth of 550–630 km is shown as a gray region. Thin broken lines represent schematic tectonic boundaries (Zeng et al., 2011). NCC: North China craton; QDSL: Qinlin-Dabie-Su-Lu fold belt; SCC: South China craton.

zone at shallow depths in the upper mantle. The same vertical structure continues further east, as far as the mantle wedge beneath the Japanese subduction zone, but the structure becomes less pronounced to the west of the leading edge of the slab (Fig. 1a). The late Cenozoic basalts (24–0.3 Ma) from the Shandong area in eastern China are located immediately above the western leading edge of the stagnant Pacific slab, and may represent the best specimens for studying geochemical traces of slab melts (Fig. 1b), because the leading edge is the oldest portion of the stagnant slab and it may have been thermally equilibrated with the ambient mantle, as suggested by seismic observations (Fig. 1a). Therefore, in order to test this hypothesis, we have compiled data and performed new analyses on the Shandong basalts.

## 2. Materials and methods

All samples were collected from lava flows with thicknesses of 5–10 m, with the exception of several scoria samples in Wudi (Fig. 2a). Fresh samples, in which olivine phenocrysts were not altered to iddingsite, were used for whole-rock analyses. Rock samples were sliced into chips using a diamond cutter, polished with a diamond grinder to remove the tracks from the cutter, and crushed into rock fragments using a rock hammer. The fragments were rinsed in an ultrasonic bath: twice with distilled water, once with acetone, and once with de-ionized water (in that order). Dried fragments were then powdered in an alumina mill. Major elemental compositions were measured using an X-ray fluorescence spectrometer (XRF, RIGAKU Simultix 12) with fused glass beads, following the method of Tani et al. (2005). Concentrations of several trace elements and rare earth elements (REEs) were analyzed by inductively coupled plasma mass spectrometry (ICP-MS, Agilent 7500ce). Pulverized whole rock samples were digested in an  $\text{HClO}_4/\text{HF}$  mixture. After drying, the samples were dissolved in  $\text{HNO}_3$ , with a small amount of HF, and In and Bi were added to the solution to conform to internal standards (Chang et al., 2003). The precision and reproducibility were generally better than 1% and 5%, respectively and the analytical results of the reference standard (JB-1a) are in good agreement with the reference values (Table S1).

The whole-rock samples were soaked at the boiling temperature of HCl (~120 °C) for 2 h in 6 N HCl, and for 30 min in a mixture of 6 N HCl and HF. They were then rinsed with deionized water at least three times (Weis et al., 2005) and dried prior to Sr–Nd–Pb–Hf isotope analyses. Sr, Nd, Pb, and Hf were isolated using Sr resin (Eichrom Industries, Illinois), Ln resin (Eichrom Industries), AG1-X8 200–400 mesh anion exchange resin, and Ln resin (Eichrom Industries), respectively. For Nd, REEs were separated initially by cation exchange chromatography (DOWEX AG50W-X8) before the use of Ln resin. The analytical procedures adopted here for chemical separation were outlined by Kimura and Nakano (2004), Hirahara et al. (2009), Miyazaki et al. (2009), Miyazaki et al. (2011), and Takahashi et al. (2009). Sr and Nd isotope ratios were measured by thermal ionization mass spectrometry (TIMS; TRITON, Thermo-Finnigan) using an instrument equipped with nine Faraday cups in a static multicollection mode. Pb and Hf isotope ratios were measured by multiple-collector (MC-)ICP-MS on a sector-type Neptune Thermo Scientific® system. Measured isotopic ratios for standard materials were as follows:  $^{87}\text{Sr}/^{86}\text{Sr} = 0.710228 \pm 10$  ( $2\sigma$ ) for NIST987;  $^{143}\text{Nd}/^{144}\text{Nd} = 0.512099 \pm 3$  ( $2\sigma$ ) for JNdi-1;  $^{206}\text{Pb}/^{204}\text{Pb} = 16.9319 \pm 10$  ( $2\sigma$ ),  $^{207}\text{Pb}/^{204}\text{Pb} = 15.4855 \pm 13$  ( $2\sigma$ ), and  $^{208}\text{Pb}/^{204}\text{Pb} = 36.6803 \pm 39$  ( $2\sigma$ ) for NIST981;  $^{179}\text{Hf}/^{177}\text{Hf} = 0.282138 \pm 16$  ( $2\sigma$ ) for JMC475. Total procedural blanks for Sr, Nd, Pb, and Hf were less than 10 pg, 5 pg, 30 pg, and 25 pg, respectively. A detailed analytical procedure is described in the supplementary material.

## 3. Results

Major and trace element abundances, isotopic compositions, and modal compositions of the phenocrysts are listed in Table 1. All discussions about major element compositions in this paper are based on

Download English Version:

<https://daneshyari.com/en/article/4698914>

Download Persian Version:

<https://daneshyari.com/article/4698914>

[Daneshyari.com](https://daneshyari.com)